# Characterization of Neutral Radicals from a Dissociative Electron Attachment Process

Zhou Li,[1,2] Aleksandar R. Milosavljević,[1,3] Ian Carmichael,[1] and Sylwia Ptasinska[1,2,*]
[1]Radiation Laboratory, University of Notre Dame, Notre Dame, Indiana 46556, USA
[2]Department of Physics, University of Notre Dame, Notre Dame, Indiana 46556, USA
[3]SOLEIL, l'Orme des Merisiers, St. Aubin, BP48, 91192 Gif sur Yvette Cedex, France
(Received 21 December 2016; published 1 August 2017)

Despite decades of gas-phase studies on dissociative electron attachment (DEA) to various molecules, as yet there has been no direct detection and characterization of the neutral radical species produced by this process. In this study, we performed stepwise electron spectroscopy to directly measure and characterize the neutrals produced upon zero-electron-energy DEA to the model molecule, carbon tetrachloride ($CCl_4$). We observed the direct yield of the trichloromethyl radical ($CCl_3^{\cdot}$) formed by DEA to $CCl_4$ and measured the appearance energies of all the other neutral species. By combining these experimental findings with high-level quantum chemical calculations, we performed a complete analysis of both the DEA to $CCl_4$ and the subsequent electron-impact ionization of $CCl_3^{\cdot}$. This work paves the way toward a complete experimental characterization of DEA processes, which will lead to a better understanding of the low-energy electron-induced formation of radical species.

DOI: 10.1103/PhysRevLett.119.053402

Low-energy electrons (<15 eV) can resonantly attach to molecules to form a short-lived transient state that quickly decays through molecular dissociation into a negative ion and neutral (radical) fragment(s). This process, commonly known as dissociative electron attachment (DEA), appears to have great significance in nature and technology, and has attracted a huge amount of scientific attention in recent decades. DEA represents a doorway for subionization and even subexcitation energy electrons to induce the decomposition of complex molecular species. Consequently, DEA studies are shedding new light on important research topics, such as radiation damage [1], and on the development of industrial applications, such as high-resolution nanolithography [2,3]. In addition, DEA is also a doorway for low-energy electrons to produce highly reactive radical species, which, themselves, play a crucial role in a variety of important biological and industrial processes. Nevertheless, despite intensive gas-phase DEA research, there has been no report of the direct detection and characterization of neutral radicals produced in DEA performed under well-defined single-collision conditions.

DEA to carbon tetrachloride ($CCl_4$) represents one of the most studied of these processes. At incident electron energies close to 0 eV, DEA to $CCl_4$ leads to the formation of only $Cl^-$ ions [4], while the other reaction product is surmised to be the trichloromethyl radical ($CCl_3^{\cdot}$),

$$e^-(E) + CCl_4 \rightarrow CCl_4^{-*} \rightarrow Cl^- + CCl_3^{\cdot}. \quad (1)$$

The intermediate anion $CCl_4^{-*}$ quickly dissociates within 5–10 ps [5]. The resonant reaction (1) attains a maximum at 0 eV with a large DEA cross section ($1.3 \times 10^{-14}$ cm$^2$ [6]), and thus represents a convenient process for our experimental investigation on the direct yield of neutral species. Moreover, $CCl_3^{\cdot}$ radicals can be efficiently produced by reaction (1) even from, e.g., presolvated electrons [7], enzymes acting as electron donors in electron transfer reactions [8], thermal electrons in plasma [9], and photoelectrons produced on surfaces (both below and above vacuum level) [10]. Therefore, reaction (1) is involved (or considered to be involved) in a number of important processes that span many distinct fields from Earth's atmospheric processes [11] to plasma applications [12,13], surface photochemistry [10,14], and toxicology [8,15,16].

To directly measure the yield of $CCl_3^{\cdot}$ radicals as a function of the electron energy $E$ upon DEA to $CCl_4$ (1), we performed stepwise electron spectroscopy (SWES) of gaseous $CCl_4$. The main rationale for using this technique was to detect neutral radical species formed through DEA by using electron impact ionization subsequent to the DEA process (see Fig. 1). In each step, we chose the desired combination of electron interaction time, ion acquisition time, and impact electron energy. Moreover, we also chose the step in which to acquire the selected ionic species.

Therefore, for each type of measurement we designed an acquisition algorithm, which we executed for the desired number of cycles, to provide data streaming from which we ultimately extracted the yield (counts per second) of the desired ionic species ($m/z$) acquired during a given step, and as a function of the electron energy in the first step ($E_1$).

For example, in the first step of the acquisition scheme [see Fig. 1(b)], the electrons at energy $E_1$ interacted with molecules in the collision region during time $t_1$, and $Cl^-$ ions (formed by DEA to $CCl_4$) were acquired during the same time window $t_1$. Therefore, by repeating this acquisition scheme at different energies $E_1$, we measured the yield of $Cl^-$ as a function of the incident electron energy $E_1$,

 

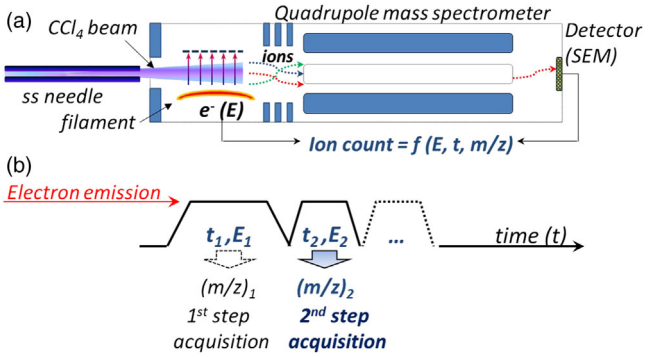


FIG. 1. SWES. (a) A schematic representation of the experimental setup. The $CCl_4$ beam ejected from a stainless-steel needle of 1 mm diameter enters the the quadrupole mass spectrometer (QMS) from the aperture on the front end. An ion source part situated at the front end of the QMS serves as the collision region, the core component of which is a metal grid cylindrical cage of 8 mm diameter and 13 mm length. The metal cage is positively biased (~3 V) to trap the cations. The electron beam is emitted from an oxide-coated iridium filament that is placed 3 mm away from the cage. The emission current was controlled at 1 $\mu$A and energy resolution is 0.5 eV [Fig. 2(a)]. The gas pressure is measured by a hot cathode ion gauge affixed to the wall of the vacuum chamber (around 0.4 m away from the reaction region). (b) A time flow of the experiment.

which represents a classical DEA experiment. The blue curve in Fig. 2(a) presents the results, which show the well-known resonance feature corresponding to the 0-eV DEA to $CCl_4$ [4,17], although it is somewhat broadened due to our lower energy resolution. It is worth noting that a

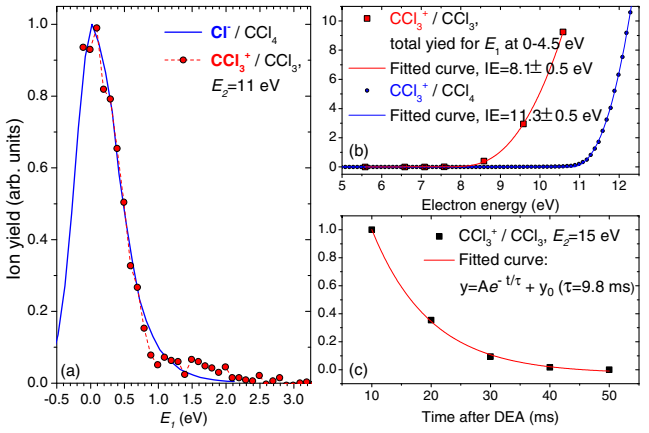


FIG. 2. *Direct observation of* $CCl_3$ *radical from DEA to* $CCl_4$. (a) Normalized ion yield of $Cl^-$ from the first-step acquisition (solid blue line) and $CCl_3^+$ from the second-step acquisition, $E_2 =$ 11 eV (red circles), as a function of the first-step incident electron energy ($E_1$). (b) Total ion yield of $CCl_3^+$ obtained for $E_1$ between 0 and 4.5 eV (red squares) as a function of the second-step incident electron energy ($E_2$), and ion yield of $CCl_3^+$ from EIF of $CCl_4$ as a function of incident electron energy, $E_1$ (blue dots). (c) Ion yield of $CCl_3^+$ as a function of the time after the first-step DEA reaction.

secondary DEA process, $e^- + CCl_3 \rightarrow Cl^- + CCl_2$, is also possible [9] during interaction time $t_1$ and also is computed to be exothermic. Nevertheless, we consider that contribution of $Cl^-$ from the secondary DEA to be negligible, based on the assumption of both a large difference in the target density between $CCl_4$ and $CCl_3$ and a very low probability of the occurrence of this two-step process under single-collision conditions.

Furthermore, we performed the two-step acquisition scheme [Fig. 1(b)], where, in the first step, electrons at energy $E_1$ interacted with molecules in the collision region during the time $t_1 = 1$ s, followed by a second step, in which electrons at energy $E_2$ interacted with molecules in the collision region during a time interval $t_2 = 0.1$ s. The $t_1$ and $t_2$ were adjusted taking into account several technical considerations, such as degradation of a filament, working at ~0 eV and at high electron emission, $CCl_3$ quenching time, time limitation needed to achieve a sufficient electron emission, and an optimal signal to noise ratio. We acquired the positive ions $CCl_3^+$ during this second step, $t_2$. Note that $CCl_3^+$ can be produced by both the electron impact fragmentation (EIF) of $CCl_4$ molecules (in the target beam) and the electron impact ionization (EI) of the $CCl_3$ radical formed in reaction (1) during time $t_1$. However, if the second-step electron energy $E_2$ is close to the ionization energy (IE) of $CCl_3$ and lower than the appearance energy (AE) of $CCl_3^+$ from EIF of $CCl_4$, this acquisition scheme allows only for the detection of the $CCl_3$ species produced in reaction (1). Therefore, by repeating this acquisition scheme at different energies $E_1$, we measured the yield of $CCl_3$ from reaction (1) as a function of the incident electron energy scanned over the DEA resonance. Since both $Cl^-$ and $CCl_3$ are formed in the same reaction, the relative ion yields obtained from the first and second-step acquisition schemes should overlap. This is indeed shown in Fig. 2(a), in which the red circles represent the yield of $CCl_3^+$ for $E_2 = 11$ eV. Note that we normalized the significantly lower intensity $CCl_3^+$ curve to that of $Cl^-$ and we calibrated the energy scale according to the decreasing slope of the $Cl^-$ curve. To the best of our knowledge, this is the first direct measurement of the resonant yield of neutral species formed by gas-phase DEA.

To verify that the $CCl_3^+$ yield presented in Fig. 2(a) originated solely from the EI of $CCl_3$, we repeated the acquisition scheme described above for different second-step energies $E_2$. Figure 2(b) presents the measured electron impact ionization yield of $CCl_3$ for $E_2$ between 6 and 11 eV (red squares), for which we estimated the yield as the total $CCl_3^+$ yield for $E_1$ at 0–4.5 eV, i.e., the area under the red curve in Fig. 2(a). For comparison, in Fig. 2(b) we plotted the yield of $CCl_3^+$ formed by the electron impact dissociation of neutral $CCl_4$ measured in the first-step acquisition scheme under the same experimental conditions (blue dots). Based on a Wannier fit [18] to the experimental data obtained in the second-step

acquisition [Fig. 2(b), red curve], we determined the IE of $CCl_3^-$ to be at $8.1 \pm 0.5$ eV. This value closely matches previously reported experimentally determined values of 8.11 [19] and 8.06 eV [20]. The uncertainty of the present IE is due to a low signal to noise ratio at the threshold and limited electron resolution. The calculated adiabatic IE of $CCl_3^-$ has been reported to be 7.954 eV [20]. Our calculations performed at the ccsd(t)/aug-cc-pVTZ level [21–24] with the Gaussian09 [25] package resulted in a vertical IE of 8.70 eV and an adiabatic IE of 8.02 eV. Note that a distinct separation between the IE of $CCl_3^-$ and the AE of $CCl_3^+$ from $CCl_4$ allows for a convenient choice of the second-step energy $E_2$ to have a reasonably high cross section for $CCl_3^-$ ionization, thus making possible efficient detection while still avoiding any interference from $CCl_4$ molecules remaining in the target beam.

We note that $CCl_3^-$ is formed only in the first-step process through reaction (1), because according to our calculations [again at the ccsd(t)/aug-cc-pVTZ level], the formation of $CCl_3^-$ from the direct C–Cl bond cleavage in $CCl_4$, $CCl_4 \rightarrow CCl_3^- + Cl$, requires an energy not less than 2.9 eV and the yield of $CCl_3^+$ seen in Fig. 2(a) appears mostly in the region $E_1 < 1$ eV. Consequently, the density of $CCl_3^-$ in the collision region should decrease in time after the completion of the first step. This was probed by the multistep SWES measurements. Figure 2(c) shows the time dependence of $CCl_3^+$ abundance, in which, after the first step in the DEA process, we set the electron energy at $E_2 =$ 15 eV and recorded the intensity of $CCl_3^+$ as output every 10 ms. Note that $E_2$ was above $CCl_3^+/CCl_4$ AE [Fig. 2(b)] to ensure high-enough $CCl_3$ detection efficiency during a short acquisition time of secondary steps. However, $CCl_3^+$ produced directly from $CCl_4$ made a constant background that was subtracted. The quenching of $CCl_3^-$ is a consequence of several processes, which cannot be resolved in the present experiment. These processes include electron interaction (ionization and fragmentation), $CCl_3^-$ interaction with the target beam, the residual gas molecules, and surrounding surfaces, and the escape of neutral radicals due to their translational kinetic energy.

In addition to the resonant yield of the $CCl_3$ radical observed from DEA to $CCl_4$ [Fig. 2(a)], we also detected all the other positive ions that can possibly originate as neutrals from $CCl_4$ fragmentation. The gas-phase DEA to $CCl_4$ at incident electron energies close to 0 eV can proceed only by reaction (1). We probed the origin of these smaller ionic fragments by determining their AEs as a function of the second-step energy $E_2$ (Fig. 3) and compared the obtained energy values to AEs and IEs for particular reactions [26–32]. The measured yields of $CCl_2^+$ and $CCl^+$ cationic fragments demonstrate that their appearance thresholds fall between the IE of the corresponding neutrals and their AE from $CCl_4$ dissociative ionization [Figs. 3(a) and 3(b)]. Therefore, these fragments can only appear from the electron impact dissociative ionization of $CCl_3^-$ formed in the DEA to $CCl_4$, which offers the first opportunity to measure AEs of these fragments from the $CCl_3$ radical. Notably, the formation of $Cl^+$ and $Cl_2^+$ occurred close to energies of the IEs of their neutrals [Figs. 3(c) and 3(d)]; therefore, these two cations result from the ionization of $Cl^-$ and $Cl_2$ rather than the EIF of $CCl_3^-$ or $CCl_4$. This is in accordance with the present calculations (Table I) showing that their enthalpies are far above experimentally probed electron energy domain.

Considering electron interaction with radicals in the gas phase, to our knowledge, only those with fluorocarbon radicals have been investigated to date, including measurements of absolute elastic cross sections for $CF_2$ and $CF_3$ [33,34] and DEA processes for $CF_2$ and $C_2F_5$ [35,36]. In the latter experiments, the target radical beam has been obtained by either pyrolysis or microwave discharge. With respect to the $CCl_3$ radical, the only relevant study was reported by Adams *et al.* [9], who used a flowing afterglow/Langmuir probe apparatus to measure a rate coefficient for a secondary process of DEA to $CCl_3^-$ formed in the primary DEA to $CCl_4$. Also, the $CCl_3$ radical has been studied, both

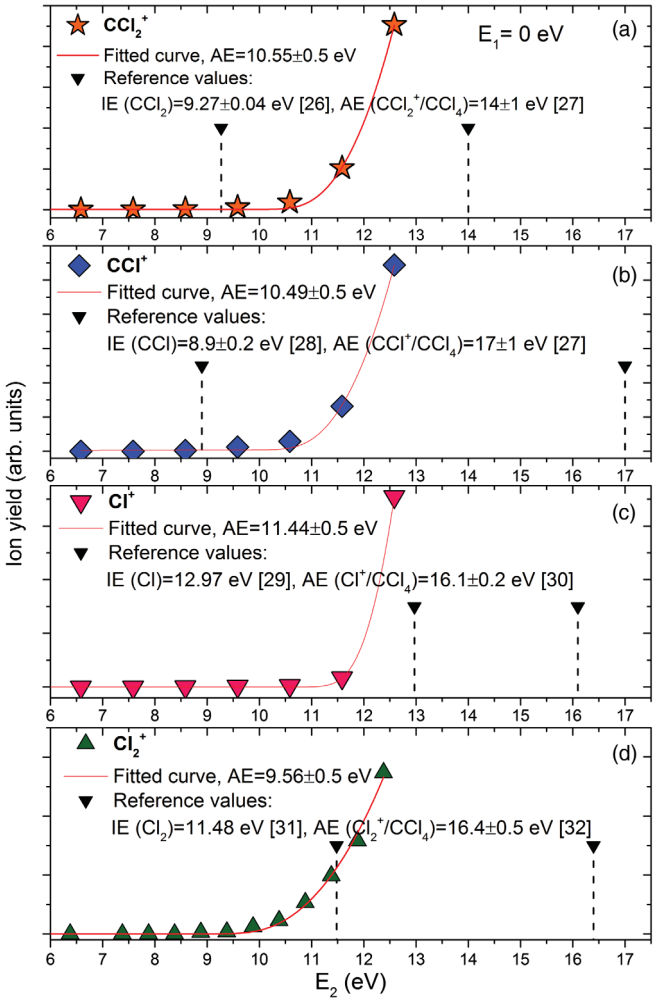


FIG. 3. *Ion yields and AEs of small cationic fragments from EIF of gas phase* $CCl_3^-$. Note: dashed lines represent experimentally determined IEs and AEs, as reported in given references.

TABLE I. Enthalpies calculated with the CBS-QB3 method at 300 K and 2500 K for different reaction pathways.

| $M^+$ | $\Delta H$ $M \rightarrow M^+ + e^-$ | | $\Delta H$ $CCl_3^{\cdot} \rightarrow M^+ + B + e^-$ | |
|---|---|---|---|---|
| | 300 K | 2500 K | 300 K | 2500 K |
| $CCl_2^+$ | 9.28 | 9.21 | 12.27 | 12.13 |
| $CCl^+$ | 8.78 | 8.77 | 12.63 | 12.46 |
| $Cl^+$ | 12.92 | 12.92 | 15.91 | 15.84 |
| $Cl_2^+$ | 11.53 | 11.53 | 15.38 | 15.22 |

theoretically and experimentally, using mass spectrometry, laser spectroscopy, and *ab initio* calculations [20,37–39]. From these calculations, electron impact IE and photon impact IE for $CCl_3^{\cdot}$ were reported previously, but no data on the EIF of $CCl_3^{\cdot}$ have been reported thus far.

Our calculations [at the ccsd(t)/aug-cc-pVTZ level] predicted the AEs of $CCl_2^+$ and $CCl^+$ from $CCl_3^{\cdot}$ at 12.01 and 12.51 eV, respectively. These energies are about 1.5 eV above the experimentally measured thresholds of $10.55 \pm 0.5$ and $10.49 \pm 0.5$ eV for $CCl_2^+$ and $CCl^+$, respectively. The deviation between the measurement and the calculation might be explained by two reasons: the region close to the filament where the reactions occurred can be of very high temperature and the parent molecule $CCl_3^{\cdot}$ resulting from the first-step DEA might be in an excited state. To estimate the effect of temperature, enthalpy changes for different pathways were calculated at various temperatures with complete basis set method CBS-QB3 [40,41] as listed in Table I. The increase in temperature from 300 to 2500 K lowers the enthalpy requirement by less than 0.2 eV, which could not explain the deviation observed in the experiment. Thus, it is more plausible that the deviation is owing to an initial excited $CCl_3^{\cdot}$ state. Previously, Popple *et al.* [5] reported the excess energy of reaction (1) to be ~0.61 eV and concluded that there is an efficient redistribution of this excess reaction energy among the internal vibrational modes of the intermediate $CCl_4^{-*}$ prior to dissociation, leaving only about 0.1 eV as a mean translational energy release.

In conclusion, we designed a SWES method to probe the $CCl_3$ radicals resulting from gas-phase DEA to $CCl_4$ around 0 eV. With this scheme, we measured the IE of $CCl_3^{\cdot}$ as well as the lifetime of $CCl_3^{\cdot}$ in vacuum conditions. We examined the cationic fragments resulting from EIF of $CCl_3^{\cdot}$ by measuring the ion yield curves of the cation fragments as a function of electron energy. By comparing the AEs and the calculated thresholds of different reaction pathways, we determined the AEs for $CCl_2^+$ and $CCl^+$ formed by the EIF of $CCl_3^{\cdot}$. The great advantage of this SWES methodology is that the production of the radicals and the subsequent ionization of the radicals can be performed in the same reaction compartment. In this way, we overcame the challenge of radical decay during transportation from the production site to the ionization site as reported in some other radical detection methods [42,43]. The method described here will have useful application in the investigation of radicals from gas-phase DEA, for which no studies have been reported. Obtaining a comprehensive picture of DEA processes has the potential to transform our understanding of the interactions of low-energy electrons with molecular systems, yielding basic science information that translates on variety biological and industrial applications.

This material is based upon work supported by the U.S. Department of Energy Office of Science, Office of Basic Energy Sciences under Award No. DE-FC02-04ER15533. This is contribution number NDRL 5161 from the Notre Dame Radiation Laboratory.

*Corresponding author.
Sylwia.Ptasinska.1@nd.edu

[1] B. Boudaïffa, P. Cloutier, D. Hunting, M. A. Huels, and L. Sanche, Science **287**, 1658 (2000).
[2] S. Engmann, M. Stano, Š. Matejčík, and O. Ingólfsson, Angew. Chem. **50**, 9475 (2011).
[3] R. M. Thorman, T. P. R. Kumar, D. H. Fairbrother, and O. Ingólfsson, Beilstein J. Nanotechnol. **6**, 1904 (2015).
[4] D. Klar, M.-W. Ruf, and H. Hotop, Int. J. Mass Spectrom. **205**, 93 (2001).
[5] R. A. Popple, C. D. Finch, K. A. Smith, and F. B. Dunning, J. Chem. Phys. **104**, 8485 (1996).
[6] S. C. Chu and P. D. Burrow, Chem. Phys. Lett. **172**, 17 (1990).
[7] C. Wang, K. Drew, T. Luo, M. Lu, and Q. Lu, J. Chem. Phys. **128**, 041102 (2008).
[8] L. G. Christophorou and D. Hadjiantoniou, Chem. Phys. Lett. **419**, 405 (2006).
[9] N. G. Adams, D. Smith, and C. R. Herd, Int. J. Mass Spectrom. Ion Process. **84**, 243 (1988).
[10] S. J. Dixon-Warren, E. T. Jensen, and J. C. Polanyi, Phys. Rev. Lett. **67**, 2395 (1991).
[11] R. J. Donovan, K. Kaufmann, and J. Wolfrum, Nature (London) **262**, 204 (1976).
[12] K. A. Föglein, P. T. Szabó, A. Dombi, and J. Szépvölgyi, Plasma Chem. Plasma Process. **23**, 651 (2003).
[13] A. Indarto, J. Choi, H. Lee, and H. Song, J. Environ. Sci. **18**, 83 (2006).
[14] S. Ryu, J. Chang, and S. K. Kim, J. Chem. Phys. **123**, 114710 (2005).
[15] L. W. D. Weber, M. Boll, and A. Stampfl, Critical reviews in toxicology **33**, 105 (2003).
[16] J. J. Kaufman, W. S. Koski, S. Roszak, and K. Balasubramanian, Chem. Phys. **204**, 233 (1996).
[17] S. Matejcik, A. Kiendler, A. Stamatovic, and T. D. Märk, Int. J. Mass Spectrom. Ion Process. **149–150**, 311 (1995).
[18] G. H. Wannier, Phys. Rev. **90**, 817 (1953).
[19] J. W. Hudgens, R. D. Johnson III, R. S. Timonen, J. A. Seetula, and D. Gutman, J. Phys. Chem. **95**, 4400 (1991).
[20] E. S. J. Robles and P. Chen, J. Phys. Chem. **98**, 6919 (1994).
[21] J. A. Pople, M. Head-Gordon, and K. Raghavachari, J. Chem. Phys. **87**, 5968 (1987).

[22] T. H. Dunning, J. Chem. Phys. **90**, 1007 (1989).
[23] R. A. Kendall, T. H. Dunning, and R. J. Harrison, J. Chem. Phys. **96**, 6796 (1992).
[24] D. E. Woon and T. H. Dunning, J. Chem. Phys. **98**, 1358 (1993).
[25] M. J. Frisch *et al.*, *Gaussian 09, Revision E.01* (Gaussian Inc., Wallingford, CT, 2009).
[26] D. W. Kohn, E. S. J. Robles, C. F. Logan, and P. Chen, J. Phys. Chem. **97**, 4936 (1993).
[27] G. R. Burton, W. F. Chan, G. Cooper, and C. E. Brion, Chem. Phys. **181**, 147 (1994).
[28] J. W. Hepburn, D. J. Trevor, J. E. Pollard, D. A. Shirley, and Y. T. Lee, J. Chem. Phys. **76**, 4287 (1982).
[29] K. Kimura, T. Yamazaki, and Y. Achiba, Chem. Phys. Lett. **58**, 104 (1978).
[30] R. E. Fox and R. K. Curran, J. Chem. Phys. **34**, 1595 (1961).
[31] A. J. Yencha, A. Hopkirk, A. Hiraya, R. J. Donovan, J. G. Goode, R. R. J. Maier, G. C. King, and A. Kvaran, J. Phys. Chem. **99**, 7231 (1995).
[32] R. F. Baker and J. T. Tate, Phys. Rev. **53**, 683 (1938).
[33] T. M. Maddern, L. R. Hargreaves, J. R. Francis-Staite, M. J. Brunger, S. J. Buckman, C. Winstead, and V. McKoy, Phys. Rev. Lett. **100**, 063202 (2008).
[34] J. R. Brunton, L. R. Hargreaves, T. M. Maddern, S. J. Buckman, G. García, F. Blanco, O. Zatsarinny, K. Bartschat, D. B. Jones, G. B. da Silva, and M. J. Brunger, J. Phys. B **46**, 245203 (2013).
[35] S. A. Haughey, T. A. Field, J. Langer, N. S. Shuman, T. M. Miller, J. F. Friedman, and A. A. Viggiano, J. Chem. Phys. **137**, 054310 (2012).
[36] T. A. Field, K. Graupner, S. Haughey, C. A. Mayhew, N. S. Shuman, T. M. Miller, J. F. Friedman, and A. A. Viggiano, J. Phys. Conf. Ser. **388**, 052086 (2012).
[37] M. Sablier and T. Fujii, Chem. Rev. **102**, 2855 (2002).
[38] M. Sablier and T. Fujii, Annu. Rep. Prog. Sect. C: Phys. Chem. **101**, 53 (2005).
[39] J. L. Holmes and F. P. Lossing, J. Am. Chem. Soc. **110**, 7343 (1988).
[40] J. A. Montgomery, M. J. Frisch, J. W. Ochterski, and G. A. Petersson, J. Chem. Phys. **110**, 2822 (1999).
[41] J. A. Montgomery, M. J. Frisch, J. W. Ochterski, and G. A. Petersson, J. Chem. Phys. **112**, 6532 (2000).
[42] N. Goldberg and H. Schwarz, Acc. Chem. Res. **27**, 347 (1994).
[43] D. R. Cyr, R. E. Continetti, R. B. Metz, D. L. Osborn, and D. M. Neumark, J. Chem. Phys. **97**, 4937 (1992).